Control Strategies for Target-Attacker-Defender Games of USVs

1st Bin Lin
Department of Automation, Shanghai Jiao Tong University
Key Laboratory of System Control and Information Processing, Ministry of Education
Shanghai 200240, PR China
fjpt-linbin@sjtu.edu.cn

2nd Lei Qiao
State Key Laboratory of Ocean Engineering, Shanghai Jiao Tong University
School of Naval Architecture, Ocean and Civil Engineering, Shanghai Jiao Tong University
Shanghai 200240, China
qiaolei@sjtu.edu.cn

3rd Zehua Jia
Department of Automation, Shanghai Jiao Tong University
Key Laboratory of System Control and Information Processing, Ministry of Education
Shanghai 200240, PR China
jiazehua@sjtu.edu.cn

4th Zhijian Sun
Department of Automation, Shanghai Jiao Tong University
CROSSOCEAN OF SUZHOU TECHNOLOGY CO., ITD
Shanghai 200240, PR China
sunzhijianfuzhou@sjtu.edu.cn

5th Min Sun
Department of Automation, Shanghai Jiao Tong University
Key Laboratory of System Control and Information Processing, Ministry of Education
Shanghai 200240, PR China
msun@sjtu.edu.cn

6th Weidong Zhang
Department of Automation, Shanghai Jiao Tong University
Key Laboratory of System Control and Information Processing, Ministry of Education
Shanghai 200240, PR China
wdzhang@sjtu.edu.cn

2021 6th International Conference on Automation, Control and Robotics Engineering (CACRE) | 978-1-6654-3576-5/21/$31.00 ©2021 IEEE | DOI: 10.1109/CACRE52464.2021.9501329

***Abstract*—This paper presents two strategies for the target-attacker-defender (TAD) game of unmanned surface vessels (USVs) with bounded velocity and angular velocity. We use nonlinear model predictive control (NMPC) to design strategies which minimize the effort for each agent to win the game. A novel R-C-S trajectory framework is proposed to evaluate the time for USVs to reach the prearranged coordinates, and is applied to both sides' strategies of the TAD game. It is assumed that strategies of both sides are unknown to each other. The attacker's strategy is based on the dynamic artificial potential field method, which guides the attacker to evasive actions according to the threat level of the defender. The strategy for the defender and the target guides the two agents to cooperate for the overall interest of the team. The performance of the proposed algorithms is tested in numerical simulations, and it turns out that the the strategies perform better than traditional methods.**

***Index Terms*—USV, target-attacker-defender game, active defense, dynamic artificial potential field**

I. Introduction

Marine robotics plays an important role in ocean exploration and exploitation. USV can carry out specific tasks to save people from extreme danger or harm, and has attracted the attention of scientists and engineers [1]. USVs are widely used in commerce, military and other fields, and research on games for multi-USV is becoming a hot issue [1, 2, 3]. Imagine a confrontational scenario of three USV players where a target is followed by a defender, then an attacker appears and is ready to hit the target while get away from the defender, what strategies can be employed for both sides to win the game? Two pursuit-evasion game problems: attacker-target and defender-attacker are contained in this scenario, and this is called as target-attacker-defender (TAD) game.

The TAD problem is usually analyzed in active aircraft defense scenarios where an aircraft launches a defending missile to intercept an attacking missile since 1976 [4]. Researches mainly focus on the strategies for the defense of the target and the defender. In [5], the command to LOS (CLOS) guidance for the defender and a cooperative guidance law for the target is proposed to keep the defender on the line joining the target and the attacker, and achieves better control effort performance. Takeshi Yamasaki [6] improves the CLOS guidance and designs a guidance law which varies according to the distance from the defender to the target and the attacker respectively. In [7], the authors provide optimal control solutions for both the defender and the target against the attacker which adopts pure pursuit (PP) and proportional navigation (PN) guidance algorithm respectively. In [8], the authors analyse the optimal cooperative strategies where dynamics of all agents are represented by arbitrary-order linear equations. In order to avoid problems caused by linearization of engagement dynamics, sliding mode control (SMC) is used to consider the strategies in nonlinear framework in [9, 10, 11]. In [12], a higher-order sliding mode (HOSM) approach is used to control the 6 degrees-of-freedom motion of the defender.

The attacker in these articles doesn't consider the threat of the defender and only intends to approach the target. In [13, 14], the authors divide the strategies of the attacker into

stages of evading the defender while ignoring the target, and pursuing the target while ignoring the defender, and present the sufficient conditions for the attacker which is faster than the defender and the target to win the game. The attacker in [15, 16] tries to get close to the target and keep away from the defender at the same time throughout the game. Authors in [17] build the intersection of the isochrones to determine the dominance regions of each agents, and provide sufficient conditions for the attacker to catch the stationary target.

Most of the above articles provide guidance strategies to control angular velocity of constant-velocity agents, and strategies are predictable to each other in those differential games. In this paper, both linear and angular velocity controls are considered, which improves the efficiency of USVs. The actions for each agent under our strategies are obtained and updated in real-time by seeking the optimal solution for objective functions. We first analyse the algorithm to derive the minimum time for a USV to reach an arbitrary area, which is of great value in pursuit-evasion games, and then we apply it to objective functions of the agents' strategies. Strategies of both sides are designed, leading the agents to minimize the effort to capture the opponent while surviving during the game. The contribution of this article is as follows.

1) We propose a near time-optimal trajectory for a USV to move from a certain position to a point with free final heading.

2 We design an attacking strategy based on dynamic artificial potential field for the attacker to approach the target while escaping the defender.

3) We design a cooperative active defense strategy for the team of the defender and the target to improve the defense efficiency.

The rest of the paper is organized as follows. In Section II, the kinematics of USV is presented and the problem is formulated. Then, a time-optimal pursuit trajectory algorithm of USV, an attacking strategy for the attacker, and a cooperative defense strategy for the defender and the target is proposed respectively in Section III. Thereafter, simulation results are conducted in Section IV to illustrate the effectiveness of the proposed strategies. Finally, conclusions are drawn in Section V.

II. PRELIMINARIES

In this section, we present the problem formulation of the TAD game for USVs. The kinematic model of players is given as

$$\begin{cases} \dot{x} &= v\cos\theta \\ \dot{y} &= v\sin\theta \\ \dot{\theta} &= \omega \end{cases} \tag{1}$$

where the state vector $X = (x, y, \theta)$ represents the Cartesian (x, y) position of the robot in the earth frame of reference and the orientation angle θ, while the input vector $U = (v, \omega)$ represents the linear speed v and the angular speed ω of the robot subject to $0 \le v \le v_{max}$, and $|\omega| \le \omega_{max}$.

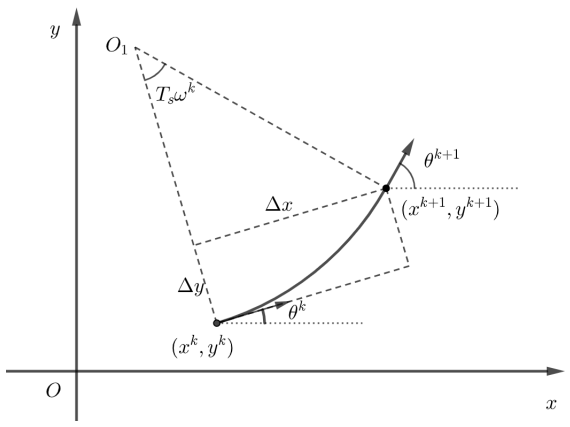

Fig. 1. Schematic diagram of robot's kinematic model

Let T_s denote the sampling time, the discrete version of the kinematic model in (1) is described as follows

$$\begin{cases} x^{k+1} &= x^k + \Delta x^k\cos\theta^k - \Delta y^k\sin\theta^k \\ y^{k+1} &= y^k + \Delta x^k\sin\theta^k + \Delta y^k\cos\theta^k \\ \theta^{k+1} &= \theta^k + T_s\omega^k \end{cases} \tag{2}$$

where Δx^k and Δy^k are shown in Fig. 1, and can be expressed as

$$\begin{cases} \Delta x^k &= \frac{v^k}{\omega^k}\sin(\omega^k T_s) \\ \Delta y^k &= \frac{v^k}{\omega^k}[1-\cos(\omega^k T_s)] \end{cases} \tag{3}$$

For the purpose of notation, we represent the discrete kinematic equations of the three agents as follows, where the symbol "T" denotes target, "A" denotes attacker and "D" denotes defender.

$$\begin{cases} X_T^{k+1} &= f_T(X_T^k, U_T^k, T_s) \\ X_A^{k+1} &= f_A(X_A^k, U_A^k, T_s) \\ X_D^{k+1} &= f_D(X_D^k, U_D^k, T_s) \end{cases} \tag{4}$$

Let r_c denote a finite radius of capture. Then the scenario that the attacker reaches the target is described as

$$\sqrt{(x_A - x_T)^2 + (y_A - y_T)^2} \le r_c \tag{5}$$

where x_A and y_A are the position coordinates of the attacker and x_T and y_T are the target's coordinates.

Similarly, the scenario under which the attacker is intercepted by the defender is described as

$$\sqrt{(x_D - x_A)^2 + (y_D - y_A)^2} \le r_c \tag{6}$$

where x_D and y_D are the position coordinates of the defender.

III. APPROACH

A. R-C-S Trajectory Framework Analysis

In order to get an algorithm to calculate the minimum time cost for a USV to reach any spot, we design an R-C-S trajectory for the USV according to kinematic model in (1).

The R-C-S trajectory consists of unions of rotation process (R), curved segment (C), and straight segment (S). Fig. 2. shows types of R-C-S trajectory for a USV to move from

point P to point E, where d denotes the straight line distance between P and E, δ represents the angle between the agent's initial heading and relative position from P to E, and r is the radius of the curved segment.

Remark 1: The R-C-S trajectory we talk about is different from the Dubins curves which is the optimal path for car-like vehicles with constant velocity and minimum turning radius. Velocity and angular velocity are both considered in R-C-S trajectory, and determine the turning radius. Rotation process is also included in R-C-S trajectory.

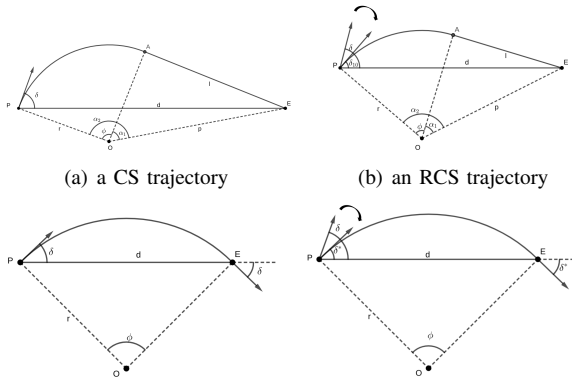

(a) a CS trajectory (b) an RCS trajectory

(c) a C trajectory (d) an RC trajectory

Fig. 2. Types of R-C-S trajectories

For the convenience of research, the R-C-S trajectory is divided into types of RCS and CS according to whether it includes the rotation process. We emphasize that one or more segments of the RCS trajectory may have zero length. For example, an RC trajectory may be thought of as an RCS trajectory. Similarly, C trajectory is a kind of CS trajectory.

The time cost of the trajectory is denoted as g_{PE}, and derive its minimum value by comparing the RCS and CS types. First we analyse CS trajectory.

Theorem 1: When $0 \leq \delta \leq \frac{\pi}{2}$, and $d \geq 2r \sin\delta$, g_{PE} of the CS trajectory has negative correlation with moving velocity v_c, angular velocity ω_c of curved segment, and speed v_l of the straight segment.

Proof: See the Appendix.

We define $r_m = \frac{v_{max}}{\omega_{max}}$, a critical angle δ_{10} described as follows

$$\delta_{10} = \arcsin \frac{d}{2r_m} \tag{7}$$

Then both trajectories are compared under certain conditions in the following theorem.

Theorem 2: When $0 \leq \delta \leq \delta_{10}$, the performance of CS and RCS tractories satisfies the following relationships:

(i) When $\delta \leq \delta_{11}$, CS trajectory costs less time then RCS trajectory.

(ii) When $\delta > \delta_{11}$, the RCS trajectory where the agent rotates from δ to δ_{11} in rotation process is the optimal R-C-S trajectory, and the critical angle δ_{11} satisfies the following equation

$$\frac{r_m \sin\delta_{11}}{d} - \sqrt{1 - \frac{2r_m \sin\delta_{11}}{d}} \cos\delta_{11} - \frac{r_m^2}{d^2} = 0 \tag{8}$$

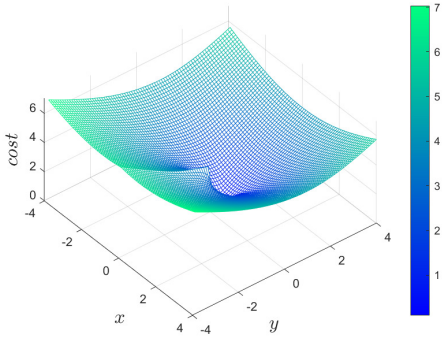

Fig. 3. Illustration of R-C-S trajectory's time cost

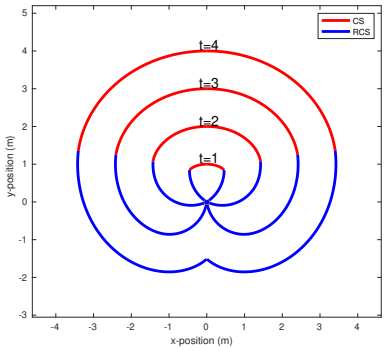

Fig. 4. Isochrones of the agent

Proof: See the Appendix.

The remaining conditions are concluded in Theorem 3.

Theorem 3: When $\delta_{10} \leq \delta \leq \pi$, RCS trajectory where the agent rotates from δ to δ_{10} in rotation process is better than CS trajectory.

Proof: See the Appendix.

The optimal time cost of R-C-S trajectory is concluded as follows

$$g_{PE}(d,\delta) = \begin{cases} \frac{\phi}{\omega_{max}} + \frac{l}{v_{max}}, & 0 \leq \delta \leq \delta_1 \\ \frac{\delta - \delta_1}{\omega_{max}} + g_{PE}(d,\delta_1), & otherwise \end{cases} \tag{9}$$

where $\delta_1 = \min\{\delta_{10}, \delta_{11}\}$, $\phi = \arccos \frac{r_m - d\cdot\sin\delta}{\sqrt{r_m^2 + d^2 - 2\cdot r_m\cdot\sin\delta}} - \arccos \frac{r_m}{\sqrt{r_m^2 + d^2 - 2\cdot r_m\cdot\sin\delta}}$, and $l = \sqrt{d^2 - 2\cdot r_m \cdot d \cdot \sin\delta}$.

Fig. 3 shows the optimal cost for an agent moving to the corresponding plane coordinates. Fig. 4 shows isochrones where the outermost isochrone corresponds to t=4s, and the time difference between successive isochrones is 1 sec. In both figures the agent moves from the origin facing the positive y-direction, and is subject to the maxium speed $v_{max} = 1m/s$ and maximum angular speed $\omega_{max} = 1rad/s$.

B. Strategy for the Attacker

The attacker's actions are obtained by solving its optimal problem. Referring to the (4), we denote $X_A^1 = (x_A^1, y_A^1, \theta_A^1)$ as the predicted statement at the next step controlled by

the input vector $U_A = (v_A, \omega_A)$. The objective function we defines is as follows

$$\min_{v_A,\omega_A} J_A(v_A, \omega_A) = g_{AT} + k_h \cdot h_{avoid} \tag{10}$$

where g_{AT} denotes the cost for the attacker to chase the target, and h_{avoid} is the cost to avoid being captured by the defender.

g_{AT} is designed as

$$g_{AT} = g_{PE}(d^1_{A1T}, \delta^1_{A1T}) \tag{11}$$

where d^1_{AT} denote the straight line distance between the attacker and the target, δ^1_{AT} denotes the angle between the attacker's initial heading and the relative position from the attacker to the target. d^1_{AT} and δ^1_{AT} can be expressed as

$$\begin{aligned} d^1_{A1T} &= \sqrt{(x^1_A - x_T)^2 + (y^1_A - y_T)^2} \\ \delta^1_{A1T} &= \theta^1_A - \arctan \tfrac{y_T - y^1_A}{x_T - x^1_A} \end{aligned} \tag{12}$$

We adopt the idea of dynamic artificial potential field algorithm to design h_{avoid}. To make the attacker prevent the defender in time when the defender approaches the attacker quickly, and avoid performing unnecessary collision avoidance maneuvers, we decompose the safety distance threshold into a fixed part r^{min}_{safe} and a variable part.

Fig. 5 illustrates the dynamic safety distance threshold of the attacker, where $\vec{d}^1_{AD}$ denotes the relative distance from the attacker's predicted position (x^1_A, y^1_A) to the defender's current position (x_D, y_D) , $\vec{v}_{AD} = \vec{v}_A - \vec{v}_D$ denotes the relative speed between the attacker's current speed $\vec{v}_A$ and the defender's maximum speed $\vec{v}_D$, and α denotes the angle between $\vec{d}^1_{AD}$ and $\vec{v}_{AD}$.

The attacker's dynamic safety distance r^A_{safe} can be expressed as

$$r^A_{safe} = r^{min}_{safe} + \frac{k_{a1}}{\omega^{max}_A + k_{a2}} \cdot \|\vec{v}_{AD}\| \cdot \cos\alpha \tag{13}$$

where r^{min}_{safe} denotes the minimum safety distance of the attacker, ω^{max}_A denotes the maximum angular speed of the attacker, $\frac{k_{a1}}{\omega^{max}_A + k_{a2}}$ signifies the attacker's ability to make a turn with the maximum angular speed ω^{max}_A, and two constants k_{a1} and k_{a2}. $\|\vec{v}_{AD}\| \cdot \cos\alpha$ is used for the attacker to increase the safety distance when the defender is approaching the attacker.

The cost function h_{avoid} is as follows

$$h_{avoid} = \begin{cases} \frac{r^A_{safe} - \|\vec{d}^1_{AD}\|}{v^{max}_A + v^{max}_D - \|\vec{v}_{AD}\|\cos\alpha + k_{b1}} + k_b \cdot \\ \quad \frac{\frac{\pi}{2} - |\alpha|}{\omega^{max}_A - \omega_A \cdot sign(\alpha) + k_{b2}}, & \|\vec{d}^1_{AD}\| \le r^A_{safe} \\ 0, & \|\vec{d}^1_{AD}\| > r^A_{safe} \end{cases} \tag{14}$$

where v^{max}_A, v^{max}_D are the maxium speed of the attacker and the defender respectively. k_b is a constant coefficient. k_{b1} and k_{b2} are positive constants. $\frac{r_{safe} - \|\vec{d}^1_{AD}\|}{v^{max}_A + v^{max}_D - \|\vec{v}\|\cos\alpha + k_{b1}}$ represents the cost for the attacker to move away from the defender by reducing approaching speed and $\frac{\frac{\pi}{2} - |\alpha|}{\omega^{max}_A - \omega_A \cdot sign(\alpha) + k_{b2}}$ is used to let the attacker change heading direction.

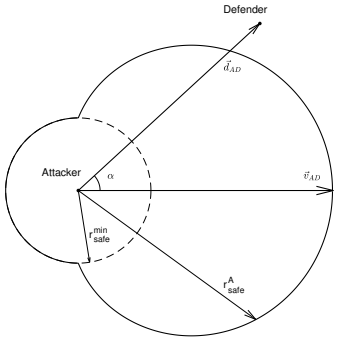

Fig. 5. Dynamic safety distance threshold of the attacker

C. Strategy for the Defender and the Target

The team of the defender and the target's controller is obtained by soling its optimal problem. The objective function is as follows

$$\min_{v_T,\omega_T,v_D,\omega_D} J_{TD}(v_T, \omega_T, v_D, \omega_D) = J_D + J_T \tag{15}$$

where J_T and J_D are the objective function of the target and the defender respectively. The input vectors $U_T = (v_T, \omega_T)$ and $U_D = (v_D, \omega_D)$ are used to predict the statements of the defener $X^1_D = (x^1_D, y^1_D, \theta^1_D)$ and the target $X^1_T = (x^1_T, y^1_T, \theta^1_T)$ at the next step referring to (4). We use the predicted statements X^1_D and X^1_T and the current statement X_A to design the cost function.

1) Defender's Strategy: The objective function of the defender is defined as

$$J_D = g_{DA} + h_{Drep} + h_{Datt} \tag{16}$$

where g_{DA} denotes the cost for the defender to capture the attacker, h_{Datt} is the cost function to attrack the defender to block the attacker's path to the target, h_{Drep} is the cost function to let the defender to avoid collision with the target in pursuit of the attacker.

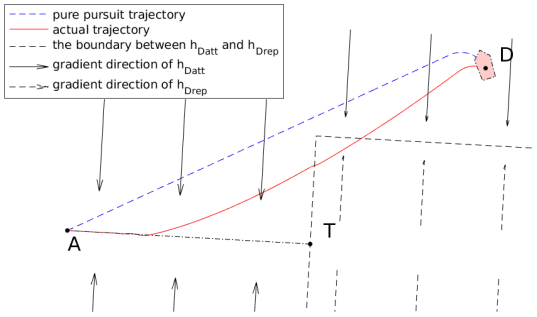

Fig. 6. Illustration of the defender's cost function

g_{DA} is expressed as

$$g_{DA} = g_{PE}(d^1_{DA}, \delta^1_{DA}) \tag{17}$$

where d^1_{DA} is the distance between the defender and the attacker as (18), δ^1_{DA} is the angle between the defender's initial heading and the relative position from the defender to the attacker as (19).

$$d^1_{DA} = \sqrt{(x^1_D - x_A)^2 + (y^1_D - y_A)^2} \tag{18}$$

$$\delta^1_{DA} = \theta^1_D - \arctan \frac{y_A - y^1_D}{x_A - x^1_D} \tag{19}$$

h_{Drep} provides repulsion for the defender when the defender appears behind the target as shown in Fig. 6 where the dashed arrows denote the gradient direction of h_{Drep} within the dashed boundary. We denote $\vec{d}^1_{TD}$ as the vector from (x^1_T, y^1_T) to (x^1_D, y^1_D), $\vec{d}_{TA}$ as the vector from (x^1_T, y^1_T) to (x_A, y_A), γ_1 as the angle between $\vec{d}^1_{TD}$ and $\vec{d}_{TA}$. h_{Drep} is expressed as

$$h_{Drep} = \begin{cases} k_{Drep} \cdot \frac{r^T_{safe} - \|\vec{d}^1_{TD}\| \cdot |\sin\gamma_1|}{v^{max}_D}, \\ \qquad \cos\gamma_1 < 0 \ \& \ \|\vec{d}^1_{TD}\| \cdot |\sin\gamma_1| \le r^T_{safe} \\ 0, \quad otherwise \end{cases} \tag{20}$$

where k_{Drep} is a constant coefficient, r^T_{safe} represents the safety distance of the target.

h_{Datt} is designed to let the defender get closer to the line between the attacker and the target, which is aimed at protecting the target. h_{Datt} is expressed as where k_{Datt} is a constant coefficient.

Fig. 6 shows the gradient direction of h_{Datt} and h_{Drep}, and the boundary between where h_{Datt} and h_{Drep} exit. The blue dashed line represents the trajectory generated when the Defender adopts the pure pursuit strategy. The red line represents the trajectory generated by the strategy we designed in this paper.

2) Target's Strategy: The target's obejective function is defined as

$$J_T = g_{Tevade} + h_{Tatt} + h_{Trep} \tag{21}$$

where g_{Tevade} represents the cost for the target to evade the attacker. h_{Tatt} is the cost function to attract the target to hide behind the defender. h_{Trep} is the cost function to avoid hitting the defender while dodging the attacker.

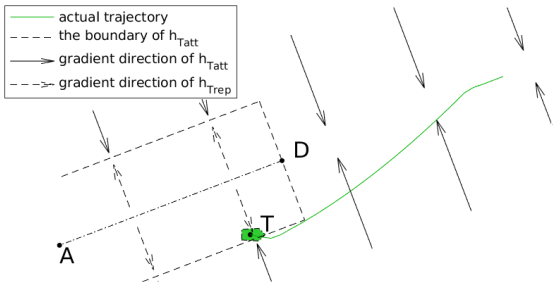

Fig. 7. Illustration of the target's cost

g_{Tevade} is expressed as

$$g_{Tevade} = -g_{PE}(d^1_{AT1}, \delta^1_{AT1}) \tag{22}$$

where d^1_{AT1} denotes the distance between the attacker and the target, δ^1_{AT1} is the angle between the attacker's initial heading and the relative position from the attacker to the target. They are expressed as follows

$$d^1_{AT1} = \sqrt{(x_A - x^1_T)^2 + (y_A - y^1_T)^2} \tag{23}$$

$$\delta^1_{AT1} = \theta_A - \arctan \frac{y^1_T - y_A}{x^1_T - x_A} \tag{24}$$

We define $\vec{d}^1_{DT}$ as the vector from (x^1_D, y^1_D) to (x^1_T, y^1_T), $\vec{d}_{DA}$ as the vector from (x^1_D, y^1_D) to (x_A, y_A), γ_2 as the angle between $\vec{d}_{DA}$ and $\vec{d}_{DT}$.

h_{Tatt} is designed to attact the target to approach the extended line of AD. h_{Tatt} can be expressed as

$$h_{Tatt} = \begin{cases} k_{Tatt} \cdot \frac{\|\vec{d}^1_{DT}\| \cdot |\sin\gamma_2| - r^D_{safe}}{v^{max}_T}, \\ \qquad \cos\gamma_2 < 0 \ || \ \|\vec{d}^1_{DT}\| \cdot |\sin\gamma_2| > r^D_{safe} \\ 0, \quad otherwise \end{cases} \tag{25}$$

h_{Trep} provides repulsion to push the target away from the connection line between the attacker and the defender. h_{Trep} is expressed as

$$h_{Trep} = \begin{cases} k_{Trep} \cdot \frac{r^D_{safe} - \|\vec{d}^1_{DT}\| \cdot |\sin\gamma_2|}{v^{max}_T}, \\ \qquad \cos\gamma_2 > 0 \ \& \ \|\vec{d}^1_{DT}\| \cdot |\sin\gamma_2| < r^D_{safe} \\ 0, \quad otherwise \end{cases} \tag{26}$$

As shown in Fig. 7, h_{Tatt} appears when the target moves outside the dashed boundary, while h_{Trep} appears when the target is inside the boundary. The green line illustrates the target's trajectory of evading the attacker and moving behind the defender.

All strategies above are based on NMPC whose proof of feasibility and convergence are given in literature [18], and the proof details are omitted here due to length limitation.

IV. SIMULATION

In this section, we use Matlab to simulate TAD games. Three scenarios are set up to present the performance of the proposed algorithm (15) for the team of the defender and the target, and the attacker's algorithm (10). The capture radius is set as $r_c = 2.5m$, the initial positions and headings of the target, the attacker and the defender are set as $(15m, -8m, 0.2\pi)$, $(-10m, 0m, -0.1\pi)$, and $(20m, 8m, -0.8\pi)$. The maximum speed and angular speed of the players are set as $v^{max}_T = 1m/s$, $\omega^{max}_T = 1rad/s$, $v^{max}_A = 2m/s$, $\omega^{max}_A = 1rad/s$, $v^{max}_D = 1$, $\omega^{max}_D = 1rad/s$.

Scenario 1: The team of the defender and the target adopts the cooperative strategy (15), and the corresponding parameters are listed in Table 1. The attacker is guided by the traditional artificial potential field method, where the safety distance is a constant value r^{min}_{safe} referring to Table 2. The result is shown in Fig. 8, where the attacker doesn't reserve enough safety distance to get away in time, and is captured by the defender. The strategy (15) and leads target to hide behind

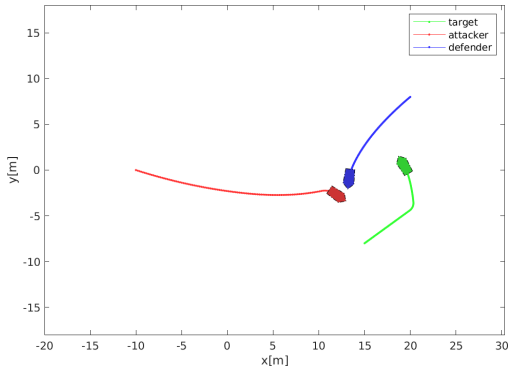

Fig. 8. Simulation result of Scenario 1

the defender, and lure the attacker to fall into the trap of the defender, which protects the target successfully.

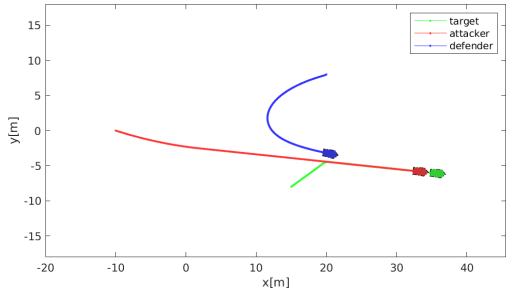

Fig. 9. Simulation result of Scenario 2

Scenario 2: The attacker's strategy is referring to the algorithm (10), with associated parameters in Table 1. The defender and the target adopt noncooperative strategy, where the objective function is expressed as

$$J_{TD} = g_{DA} + g_{Tevade} \tag{27}$$

where g_{DA} and g_{Tevade} are described in (17) and (22), and parameters are listed in Table 2. Fig. 9 illustrates the simulation result where the defender fails to intercept the attacker, and the target is caught finally. Guided by the proposed algorithm, the attacker estimates the defender's threat, and pursues the target with minimum effort.

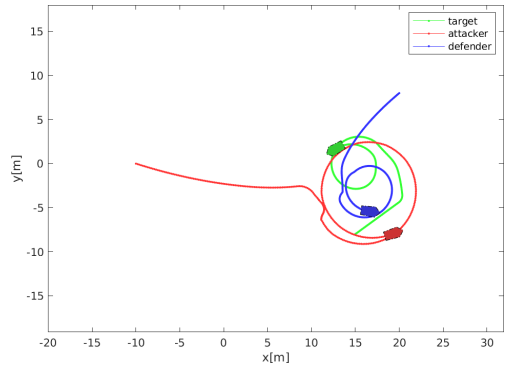

Fig. 10. Simulation result of Scenario 3

Scenario 3: The attacker adopts the algorithm (10) while the team of the defender and the target adopts the algorithm (15). The parameters of each team are shown in Table 1. Fig. 10 shows the result of the game where the target is hiding behind the defender and the attacker is trying to pursuit the target while avoiding the defender from approaching the attacker. Both sides tend to an equilibrium state.

TABLE I
SIMULATION PARAMETERS OF THE PROPOSED ALGORITHMS

Parameter	Symbol	Value
repulsive cost coefficient of the defender	k_{Drep}	**1**
attractive cost coefficient of the defender	k_{Datt}	**2**
repulsive cost coefficient of the target	k_{Trep}	**1**
attractive cost coefficient of the target	k_{Tatt}	**2**
safety distance coefficient of the attacker	$\frac{k_{a1}}{\omega_A^{max}+k_{a2}}$	$\frac{2}{\omega_A^{max}+1}$
minimum safety distance of the attacker	r_{safe}^{min}	**4**
speed constant of the attacker	k_{b1}	**1**
angular speed constant of the attacker	k_{b2}	**1**
angular speed cost coefficient of the attacker	k_b	**10**
avoidance cost coefficient of the attacker	k_h	**10**

TABLE II
SIMULATION PARAMETERS OF CONTROL GROUP'S STRATEGY

Parameter	Symbol	Value
minimum safety distance of the attacker	r_{safe}^{min}	**4**
speed constant of the attacker	k_{b1}	**1**
angular speed constant of the attacker	k_{b2}	**1**
angular speed cost coefficient of the attacker	k_b	**10**
avoidance cost coefficient of the attacker	k_h	**10**

V. CONCLUSION

In this paper, novel strategies are proposed for both sides of the target-attacker-defender game for USVs. NMPC is used to control and update actions for each agent with the optimal benefits. To evaluate minimum time it takes for USVs to reach the destination, we propose a novel R-C-S trajectory framework referring to the kinematic of the USV. Guided by the proposed attacking strategy, the attacker evades the defender according to the level of threat, and improves the efficiency of pursuing the target in the meanwhile. The defender and the target cooperate for the common goal to protect the target and expel the attacker under the strategy for the target-defender group. The simulation results show that both strategies are effective, and have better performance than the existing algorithms.

VI. ACKNOWLEDGEMENTS

This paper is partly supported by the National Science Foundation of China (61627810), National Key R&D Program of China (2017YFE0128500), Key R&D Program of Guangdong (2020B1111010002), Shanghai Sailing Program under Grant 21YF1419800, State Key Laboratory of Ocean Engineering (Shanghai Jiao Tong University) under Grant GKZD010081, and LingChuang Research Project of China National Nuclear Corporation.

APPENDIX

A. Proof of Theorem 1

Proof: The radius of the curved segment can be expressed as

$$r = \frac{v_c}{\omega_c} \tag{28}$$

The time cost of the trajectory is described as

$$g_{PE} = \frac{\phi}{\omega_c} + \frac{l}{v_s} \tag{29}$$

where $\phi = \arccos \frac{r - d\cdot\sin\delta}{\sqrt{r^2+d^2-2\cdot r\cdot\sin\delta}} - \arccos \frac{r}{\sqrt{r^2+d^2-2\cdot r\cdot\sin\delta}}$, and $l = \sqrt{d^2 - 2\cdot r\cdot d\cdot\sin\delta}$

Obviously, g_{PE} is inversely proportional to ω_c and v_s.

Then mathematical relation between g_{PE} and r is discussed below.

$$\frac{\partial g_{PE}}{\partial r} = -\frac{d\cdot\cos\delta}{r^2+d^2-2\cdot r\cdot d\cdot\sin\delta}\cdot\frac{1}{\omega_c} - \frac{d\cdot\sin\delta}{\sqrt{d^2-2\cdot r\cdot d\cdot\sin\delta}}\cdot\frac{1}{v_c} + \frac{d^2 - r\cdot d\cdot\sin\delta}{\sqrt{d^2-2\cdot r\cdot d\sin\delta}(r^2+d^2-2\cdot r\cdot d\cdot\sin\delta)}\cdot\frac{1}{\omega_c} \tag{30}$$

Let $k = \sqrt{1 - \frac{2\cdot r\cdot\sin\delta}{d}}$, and it is subject to $0 \le k \le 1$, due to $d \ge 2r\sin\delta$.

Let $u = \cos\delta$, and it is subject to $0 \le u \le 1$, due to $0 \le \delta \le \frac{\pi}{2}$.

Define $A = \sqrt{1 - \frac{2\cdot r\cdot\sin\delta}{d}}\left(\frac{r^2}{d^2} + 1 - \frac{2\cdot r\cdot\sin\delta}{d}\right)\cdot r\cdot\sin\delta\cdot\omega_c$, and it is easy to know that $A \ge 0$.

Define $F = \frac{\partial g_{PE}}{\partial r}\cdot A$, then

$$\frac{\partial F}{\partial u} = \frac{1}{2}k\left(4k\cdot u + k^2 - 1\right) \tag{31}$$

If $\sqrt{5} - 2 \le k \le 1$, F increases with rise of u when $u \in [0, \frac{1-k^2}{4k}]$, and decreases rise of when $u \in [\frac{1-k^2}{4k}, 1]$.

If $0 \le k < \sqrt{5} - 2$, F decreases with rise of u when $u \in [0, 1]$.

So $F_{max} = \max\{F(u=0), F(u=1)\}$.

Due to that

$$F(u=0) = -\frac{1}{2}k^2\left(k^2+1\right) \le 0 \tag{32}$$

$$F(u=1) = -\frac{1}{2}k(k^2-1)(k-1) \le 0 \tag{33}$$

we can conclude that $F \le 0$, and $\frac{\partial g_{PE}}{\partial r} \le 0$.

As a result, g_{PE} decreases with rise of r, and has negative correlation with v_c due to the fact that v_c is proportional to r.

B. Proof of Theorem 2

Proof: An RCS trajectory can be regarded as the union of a rotation process and a CS trajectory.

The time cost can be expressed as

$$g_{PE} = \frac{\delta - \delta^*}{\omega_r} + \frac{\phi}{\omega_c} + \frac{l}{v_c} \tag{34}$$

where ω_r is the angular velocity of the rotation segment.

According to theorem 1, time cost of the CS part is shortest when $\omega_c = \omega_{max}$, and $v_c = v_{max}$, and corresponding radius is $r = r_m$.

So the optimal g_{PE} is described as

$$g_{PE} = \frac{\delta - \delta^*}{\omega_{max}} + \frac{\phi}{\omega_{max}} + \frac{l}{v_{max}} \tag{35}$$

where $\phi = \arccos \frac{r_m - d\cdot\sin\delta^*}{\sqrt{r_m^2+d^2-2\cdot r_m\cdot\sin\delta^*}} - \arccos \frac{r_m}{\sqrt{r_m^2+d^2-2\cdot r_m\cdot\sin\delta^*}}$, and $l = \sqrt{d^2 - 2\cdot r_m\cdot d\cdot\sin\delta^*}$.

Then take the derivative of g_{PE}

$$\frac{\partial g_{PE}}{\partial\delta^*} = -\frac{r_m\cdot d\cos\delta^*}{\sqrt{d^2-2r_m\cdot d\cdot\sin\delta^*}}\cdot\frac{1}{v_{max}} - \frac{1}{\omega_{max}} + \frac{1}{\omega_{max}}\cdot \left[\frac{d^2 - d\cdot r_m\cdot\sin\delta^*}{r_m^2+d^2-2r_m\cdot d\cdot\sin\delta^*} + \frac{r_m^2 d\cos\delta}{\sqrt{d^2-2r_m\cdot d\cdot\sin\delta}\cdot(r_m^2+d^2-2r_m\cdot d\cdot\sin\delta^*)}\right] \tag{36}$$

Let $B = \frac{d^2+r^2-2r\cdot d\cdot\sin\delta^*}{d^2}\cdot\omega_{max}$, and it is easy to know that $B \ge 0$.

Define $G = \frac{\partial g}{\partial\delta^*}\cdot B$, and we can get that

$$\frac{\partial G}{\partial\delta^*} = \sqrt{1 - \frac{2r_m\sin\delta^*}{d}}\sin\delta^* + \frac{r_m\cos^2\delta^*}{\sqrt{d^2-2r_m d^2\sin\delta^*}} + \frac{r_m}{d}\cos\delta^* \ge 0 \tag{37}$$

$$G(\delta^*=0) = -1 - \frac{r_m^2}{d^2} \le 0 \tag{38}$$

$$G(\delta^* = \frac{\pi}{2}) = \frac{r_m}{d} - \frac{r_m^2}{d^2} > 0 \tag{39}$$

According to (8), $G(\delta_{11}) = 0$.

As a result, if $\delta_{11} < \delta$, g_{PE} decreases with rise of δ^* when $\delta^* \in (0, \delta_{11})$, and g_{PE} increases with rise of δ^* when $\delta^* \in (\delta_{11}, \delta)$, then the RCS trajectory where then agent rotates from δ to δ_{11} in rotation segment is the optimal R-C-S trajectory. If $\delta_{11} > \delta$, then g_{PE} decreases with δ^* increasing from 0 to δ, and the CS trajectory is better than RCS trajectory.

C. Proof of Theorem 3

Proof: Given that $\delta \ge \delta_{10}$, so $r \le \frac{d}{2\sin\delta}$. According to theorem 1, the optimal g_{PE} of CS trajectory corresponds to the condition that $\omega_c = \omega_{max}$, and $r = \frac{d}{2\sin\delta}$, then the length of the straight segment is zero as Fig.2 (c), g_{PE} is expressed as

$$g_{PE} = \frac{2\delta}{\omega_{max}} \tag{40}$$

When $\delta_{10} \le \delta^* < \delta$, CS part of the optimal RCS trajectory has the straight segment $l = 0$, and g_{PE} of the optimal RCS is described as

$$g_{PE} = \frac{\delta + \delta^*}{\omega_{max}} \tag{41}$$

As a result, the RCS trajectory costs less time than the CS trajectory.

REFERENCES

[1] Y. Cheng, Z. Sun, Y. Huang, and W. Zhang, "Fuzzy categorical deep reinforcement learning of a defensive game for an unmanned surface vessel," *International Journal of Fuzzy Systems*, vol. 21, no. 2, pp. 592–606, 2019.

[2] E. Simetti, A. Turetta, S. Torelli, and G. Casalino, "Civilian harbour protection: Interception of suspect vessels with unmanned surface vehicles," *IFAC Proceedings Volumes*, vol. 45, no. 27, pp. 435–440, 2012.

[3] Z. Peng, Y. Jiang, and J. Wang, "Event-triggered dynamic surface control of an underactuated autonomous surface vehicle for target enclosing," *IEEE Transactions on Industrial Electronics*, vol. 68, no. 4, pp. 3402–3412, 2020.

[4] R. L. Boyell, "Defending a moving target against missile or torpedo attack," *IEEE Transactions on Aerospace and Electronic Systems*, no. 4, pp. 522–526, 1976.

[5] A. Ratnoo and T. Shima, "Line-of-sight interceptor guidance for defending an aircraft," *Journal of Guidance, Control, and Dynamics*, vol. 34, no. 2, pp. 522–532, 2011.

[6] T. Yamasaki, S. Balakrishnan, and H. Takano, "Modified command to line-of-sight intercept guidance for aircraft defense," *Journal of Guidance, Control, and Dynamics*, vol. 36, no. 3, pp. 898–902, 2013.

[7] E. Garcia, D. W. Casbeer, and M. Pachter, "Cooperative strategies for optimal aircraft defense from an attacking missile," *Journal of Guidance, Control, and Dynamics*, vol. 38, no. 8, pp. 1510–1520, 2015.

[8] T. Shima, "Optimal cooperative pursuit and evasion strategies against a homing missile," *Journal of Guidance, Control, and Dynamics*, vol. 34, no. 2, pp. 414–425, 2011.

[9] S. R. Kumar and D. Mukherjee, "Cooperative guidance strategies for active aircraft protection," in *2019 American Control Conference (ACC)*. IEEE, 2019, pp. 4641–4646.

[10] S. R. Kumar and T. Shima, "Cooperative nonlinear guidance strategies for aircraft defense," *Journal of Guidance, Control, and Dynamics*, vol. 40, no. 1, pp. 124–138, 2017.

[11] A. Sinha and S. R. Kumar, "Supertwisting control-based cooperative salvo guidance using leader–follower approach," *IEEE Transactions on Aerospace and Electronic Systems*, vol. 56, no. 5, pp. 3556–3565, 2020.

[12] T. Yamasaki and S. N. Balakrishnan, "Terminal intercept guidance and autopilot for aircraft defense against an attacking missile via 3d sliding mode approach," in *2012 American Control Conference (ACC)*. IEEE, 2012, pp. 4631–4636.

[13] S. Rubinsky and S. Gutman, "Three body guaranteed pursuit and evasion," in *AIAA guidance, navigation, and control conference*, 2012, p. 4910.

[14] ——, "Three-player pursuit and evasion conflict," *Journal of Guidance, Control, and Dynamics*, vol. 37, no. 1, pp. 98–110, 2014.

[15] M. Weiss, T. Shima, D. Castaneda, and I. Rusnak, "Combined and cooperative minimum-effort guidance algorithms in an active aircraft defense scenario," *Journal of Guidance, Control, and Dynamics*, vol. 40, no. 5, pp. 1241–1254, 2017.

[16] L. Liang, Z. Peng, F. Zhang, and X. Li, "Two coupled pursuit-evasion games in target-attacker-defender problem," in *2017 IEEE 56th Annual Conference on Decision and Control (CDC)*. IEEE, 2017, pp. 5596–5601.

[17] M. Coon and D. Panagou, "Control strategies for multiplayer target-attacker-defender differential games with double integrator dynamics," in *2017 IEEE 56th Annual Conference on Decision and Control (CDC)*. IEEE, 2017, pp. 1496–1502.

[18] L. Grüne and J. Pannek, *Nonlinear Model Predictive Control: Theory and Algorithms*, 01 2017.